Observation of Genuine Three-Photon Interference

Sascha Agne,[1,*] Thomas Kauten,[2] Jeongwan Jin,[1] Evan Meyer-Scott,[1,3] Jeff Z. Salvail,[1]
Deny R. Hamel,[4] Kevin J. Resch,[1] Gregor Weihs,[2,5] and Thomas Jennewein[1,5,†]

[1]*Institute for Quantum Computing and Department of Physics and Astronomy, University of Waterloo,
Waterloo, Ontario N2L 3G1, Canada*
[2]*Institut für Experimentalphysik, Universität Innsbruck, Technikerstraße 25, 6020 Innsbruck, Austria*
[3]*Department of Physics, University of Paderborn, Warburger Straße 100, 33098 Paderborn, Germany*
[4]*Département de Physique et d'Astronomie, Université de Moncton, Moncton, New Brunswick E1A 3E9, Canada*
[5]*Quantum Information Science Program, Canadian Institute for Advanced Research, Toronto, Ontario M5G 1Z8, Canada*
(Received 17 October 2016; published 10 April 2017)

Multiparticle quantum interference is critical for our understanding and exploitation of quantum information, and for fundamental tests of quantum mechanics. A remarkable example of multi-partite correlations is exhibited by the Greenberger-Horne-Zeilinger (GHZ) state. In a GHZ state, three particles are correlated while no pairwise correlation is found. The manifestation of these strong correlations in an interferometric setting has been studied theoretically since 1990 but no three-photon GHZ interferometer has been realized experimentally. Here we demonstrate three-photon interference that does not originate from two-photon or single photon interference. We observe phase-dependent variation of three-photon coincidences with $(92.7 \pm 4.6)\%$ visibility in a generalized Franson interferometer using energy-time entangled photon triplets. The demonstration of these strong correlations in an interferometric setting provides new avenues for multiphoton interferometry, fundamental tests of quantum mechanics, and quantum information applications in higher dimensions.

In 1989, Franson [1] considered a light source that emits two photons simultaneously but at an unknown absolute time. These photon pairs, when sent through identical, but independent, unbalanced interferometers, display interference in the twofold coincidence rate, but not in the independent single detection rates [2]. This is the simplest manifestation of what we call genuine interference: certain multipartite entangled quantum states display correlations in the highest order with interference that cannot be explained by lower-order interference [3–5]. The Franson interferometer is representative of a class of two-particle interferometers that convert continuous-variable entanglement into two-valued observables via the two output ports of an interferometer [6]. Accordingly, with three independent interferometers, three continuously entangled photons can show genuine interference as well. This is known as the GHZ interferometer [4,7–9] and is shown schematically in Fig. 1(a). However, multiphoton entanglement experiments are considered less challenging when using polarization [10] and only Mermin's "three-spin gadget" [11] has been realized [12] rather than the three-photon GHZ interferometer. Such an interferometer differs from previously realized NOON-type interferometers, where the photons are manipulated together in a single interferometer to show superresolution effects with, in general, nonzero lower-order interference [3,9,13,14].

Energy-time entangled photon triplets can be described by a continuous superposition of triplet creation times [9],

$$|\Psi\rangle_{\text{triplet}} = \int dt\, a_1^\dagger(t) a_2^\dagger(t) a_3^\dagger(t) |0\rangle. \tag{1}$$

We let each photon individually propagate through an unbalanced interferometer with a time difference $\tau = 3.7$ ns between the short and long arm, as shown in Fig. 1(a). The creation operators in Eq. (1) can be expressed in terms of the detection modes A_n and B_n ($n = 1, 2, 3$) as

$$a_n^\dagger(t) = \frac{1}{2}[A_n^\dagger(t) + iB_n^\dagger(t)] - \frac{e^{i\varphi_n}}{2}[A_n^\dagger(t+\tau) + iB_n^\dagger(t+\tau)]. \tag{2}$$

The detection modes correspond to the complementary interferometer output modes and thus partition the eight possible detector combinations into even or odd parity sets

$$AAA = \{A_1A_2A_3, A_1B_2B_3, B_1A_2B_3, B_1B_2A_3\},$$
$$BBB = \{B_1B_2B_3, B_1A_2A_3, A_1B_2A_3, A_1A_2B_3\}. \tag{3}$$

Using detectors with ~ 1 ns time resolution, sufficiently shorter than the interferometer path difference, we can detect three photons simultaneously, selecting, for example, for $A_1A_2A_3$ coincidences, the output state [9]

$$|\Psi\rangle_{A_1A_2A_3} \propto \left[1 - \exp\left(i\sum_{n=1}^{3}\varphi_n\right)\right] \int dt \prod_{n=1}^{3} A_n^\dagger(t)|0\rangle. \tag{4}$$

From these we obtain the three-photon coincidence probabilities for the AAA $(-)$ and BBB $(+)$ combinations

$$P_3 = \frac{1}{2}[1 \pm \cos(\varphi_1 + \varphi_2 + \varphi_3)]. \quad (5)$$

Thus, the three-photon coincidence rate depends on the sum of the interferometer phases. Moreover, one can also show that the single photon and two-photon coincidence rates are constant by calculating the marginal probabilities [8]. This result corresponds to the third photon carrying time information about the other two photons and "tracing it out" will erase any interference between the pair.

The main experimental challenge in observing higher-order interference is posed by the low generation efficiency of multipartite entangled states. The count rate in our experiment is critical since losses in the interferometers scale with the number of photons and only one-quarter of the transmitted photon triplets contribute to the interference term, as is evident from Fig. 1(b). Among the alternatives for the direct generation of photon triplets are $\chi^{(3)}$ interaction in optical fibers [15], sum-frequency generation of energy-time entangled photon pairs [16], and cascaded spontaneous parametric down-conversion (CSPDC) [17]. We employ a newly designed CSPDC source that produces photon triplets at a high rate in a state that approximates the triplet state in Eq. (1). Given that the 404 nm pump coherence length is much longer than the interferometer path difference, the emitted photon triplet will display interference in the threefold coincidences shown in Eq. (5). The full experimental setup that we use to achieve sufficiently low losses to compile robust measurement statistics is shown in Fig. 2. Additional details, including
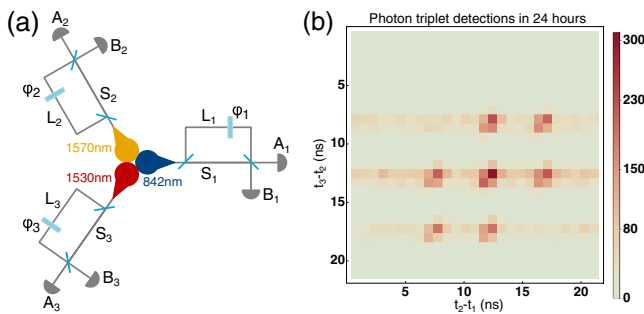

FIG. 1. Three-photon Franson interferometer. (a) Each of three energy-time entangled photons (at wavelengths 842, 1530, and 1570 nm) travels through an unbalanced interferometer with a path difference τ between the short (S) and long (L) paths. (b) The measured arrival time difference histogram with a bin size of 0.78 ns and peak separation of $\tau = 3.7$ ns displays seven narrow peaks corresponding to the eight possible path combinations $S_1S_2S_3$, $L_1S_2S_3$, $S_1L_2S_3$, $S_1S_2L_3$, $L_1L_2S_3$, $L_1S_2L_3$, $S_1L_2L_3$, and $L_1L_2L_3$. When all three photons take either the short or the long path the relative arrival time is the same, so the $S_1S_2S_3$, and $L_1L_2L_3$ events overlap, forming the central peak. This overlap is a coherent superposition, leading to a three-photon coincidence rate that depends on the phases φ_n ($n = 1, 2, 3$).

spectra of photon triplets can be found in Secs. I and III of Ref. [18].

We first record photon events for 12 phase settings of the 1570 nm photons by changing the angles of the glass phase plate in the 1570 nm long arm. Measuring for 2 h per angle, over 24 h we detect 4648 triplets within a coarse 20 ns coincidence window. The histogram in Fig. 1(b) shows the distribution of arrival times with seven peaks that reflect the eight possible path combinations. With a bin size of 0.78 ns in both dimensions, we have 309 triplets in the central bin and an average of 137 triplets in each of the six highest side bins. The triplets in the central bin are shown as a function of the 1570 nm phase in Fig. 3(a) and fits of Eq. (5) yield visibilities $V_{AAA} = (92.8 \pm 6.6)\%$ and $V_{BBB} = (92.7 \pm 6.4)\%$. This gives an average visibility of $(92.7 \pm 4.6)\%$ without background subtraction (the visibility estimation procedure is discussed in Sec. IV of Ref. [18]), which is above the classical visibility bound of 50% for genuine three-photon interference [20,21].

As shown in Figs. 3(b) and 3(c), the two-photon coincidences and single count rates from the same data set display only small drifts in count rates over the course
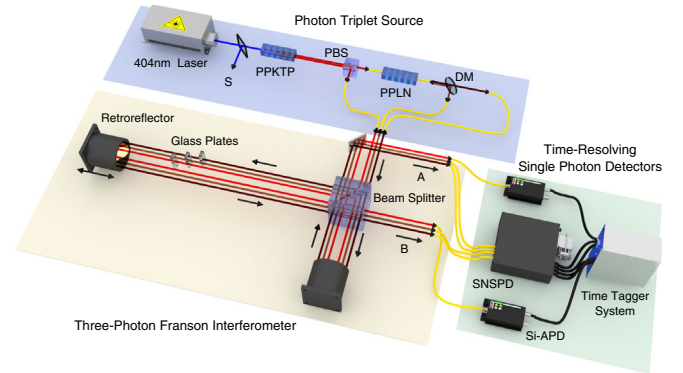

FIG. 2. Experimental setup for the observation of genuine three-photon interference. A continuous-wave grating-stabilized laser diode (404 nm, 43 mW, >25 m coherence length) pumps a 25 mm periodically poled potassium titanyl phosphate (PPKTP) crystal to generate pairs of 842/776 nm photons in type-II down-conversion, which are split at a polarizing beam splitter (PBS). The 776 nm photons pump a periodically poled lithium niobate (PPLN) waveguide to generate 1530/1570 nm photon pairs in type-0 down-conversion. These infrared photons are split in free-space by a dichroic mirror (DM) before entering the three-photon Franson interferometer, which is realized as three spatial modes of a single interferometer with a path difference $\tau = 3.7$ ns. Photon phase control is achieved with motorized glass plates. At the two output ports A and B, the 842 and 1530/1570 nm photons are detected with free-running silicon avalanche photodiodes (Si-APD) and superconducting nanowire single photon detectors (SNSPD), respectively, and their arrival time is registered with a time tagger system. All fibers (yellow) are single-mode fibers at respective wavelengths. A few pump photons are picked off and sent through another interferometer path (S—not drawn) for interferometer stabilization (see Sec. I of Ref. [18]).
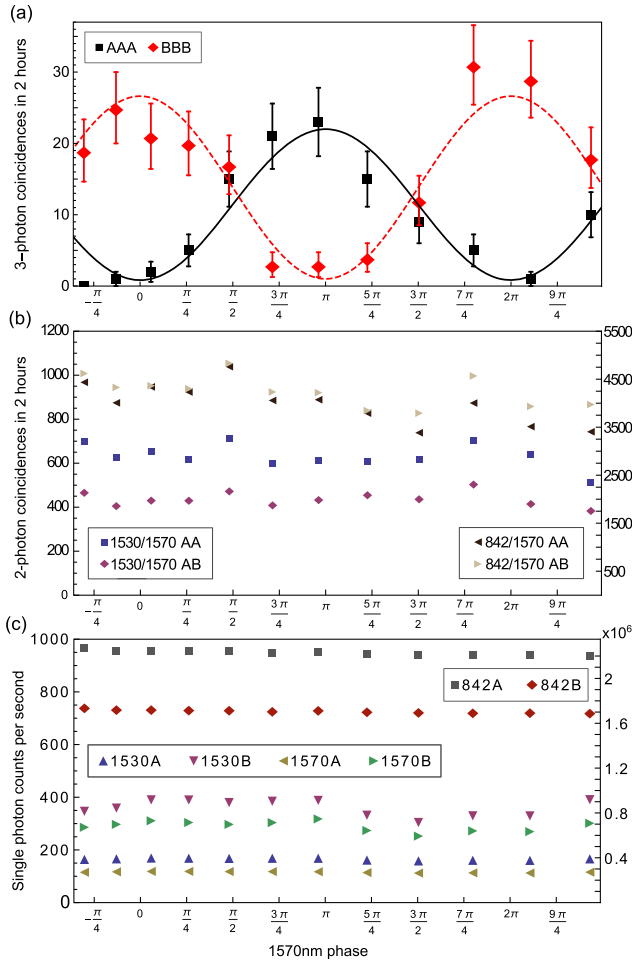
FIG. 3. Three-photon coincidences, two-photon coincidences, and single photon counts in our three-photon Franson interferometer. The measured three-photon coincidences (a) show clear signature of interference with an average visibility of $(92.7 \pm 4.6)\%$ without background subtraction. The error bars are approximated by Poissonian count errors. No systematic modulation is visible in the measured (b) two-photon coincidences that can lead to a triplet in the histogram Fig. 1(b) and (c) single detection rates. The letters in the legend of the twofold coincidences indicate the set of detector combinations. For example, 1530/1570 AA is the sum of 1530/1570 coincidences in detector combinations $A_2 A_3$ and $B_2 B_3$. The shown single detection rates for the 1530/1570 nm photons are dominated by dark counts of the SNSPDs, while the 842 nm dark counts (Si-APDs, ~ 2400 per sec) are negligible.

of the experiment but no systematic, complementary modulation. We observe no two-photon Franson interference of 1530/1570 nm photons because the coherence length of the 776 nm photons as a pump for the second SPDC process is much smaller than the interferometer path difference (the spectra can be found in Sec. III of Ref. [18]). Variations in the two-photon coincidences can be due to fluctuations in the mean SNSPD dark count rate, which affects the observed threefold coincidences. For example, comparing Figs. 3(a) and 3(b) at the fifth ($\approx \pi/2$) and ninth ($\approx 3\pi/2$) data point we see that the higher threefold

coincidences agree with an isolated increase in twofold coincidences. Note that whereas the infrared singles are dominated by dark counts, the ratio of signal to dark counts per second in the Si-APDs is $\sim 10^5$ and therefore any modulation present in the 842 nm single counts would be clearly visible.

In a second measurement, we scan the phase of 1530 nm photons. Figure 4(a) shows the result of a scan in which the 1530 nm glass phase plate is pretilted so that two fringes are observed over 2.2 degrees. The three-photon interference average visibility is $(84.6 \pm 6.3)\%$ [$V_{AAA} = (77.9 \pm 7.9)\%$ and $V_{BBB} = (91.4 \pm 9.9)\%$] without background subtraction. The visibility difference between AAA and BBB curves is consistent with statistical errors that we observe when generating Monte Carlo data sets for visibility error estimation. The phase of 842 nm photons is scanned in a third measurement. Given that the wavelength is about half the other photon's wavelengths and the glass plates have identical thicknesses, we expect a full three-photon interference fringe over half the 1570 nm scan range. Indeed, as Fig. 4(b) shows, we observe a fringe with $(84.6 \pm 4.1)\%$ average visibility ($V_{AAA} = (82.9 \pm 6.4)\%$ and $V_{BBB} = (86.3 \pm 5.2)\%$) without background subtraction. As for the 1570 nm phase scan, the two-photon coincidences and single detection rates show no modulation for both the 1530 and 842 nm phase scans. In a last series of measurements, we block individual or all interferometer
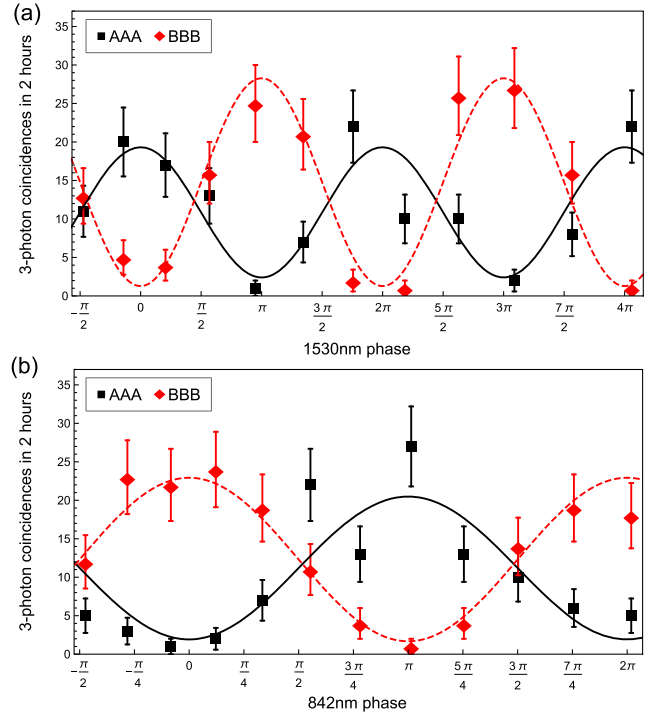

FIG. 4. The phase scan for (a) 1530 and (b) 842 nm photons of photon triplets provide further evidence for genuine three-photon interference, yielding average interference visibilities of $(84.6 \pm 6.3)\%$ and $(84.6 \pm 4.1)\%$, respectively.

paths and record photon events. As expected, the three-photon coincidences are no longer phase-sensitive, demonstrating that the modulation with all interferometer paths open is due to interference (a detailed discussion is given in Sec. V of Ref. [18]).

We have experimentally shown that genuine three-photon interference is accessible with energy-time entangled photon triplets. Such states and the new quantum interference phenomena they exhibit suggest several interesting directions for future research. Using a pulsed pump, our experimental apparatus should be able to generate and analyze three-photon time-bin states [22] for direct implementations of quantum communication protocols [23]. Our setup could be converted to perform NOON-style interferometry with applications in phase superresolution and supersensitivity [9]. Furthermore, this system could be used for fundamental questions of nonlocality [24] in tests of both Mermin [25] and Svetlichny inequalities [26], more detailed study on the three-photon joint-spectral function [27], and enable the realization and study of genuine tripartite hyperentanglement [28].

Note added in proof.—We recently became aware of a different approach to study genuine three-photon interference using three independent photons [29].

---

*sascha.agne@uwaterloo.ca
†thomas.jennewein@uwaterloo.ca

[1] J. D. Franson, Phys. Rev. Lett. **62**, 2205 (1989).
[2] P. G. Kwiat, A. M. Steinberg, and R. Y. Chiao, Phys. Rev. A **47**, R2472 (1993).
[3] J. W. Pan, Z. B. Chen, C. Y. Lu, H. Weinfurter, A. Zeilinger, and M. Zukowski, Rev. Mod. Phys. **84**, 777 (2012).
[4] D. M. Greenberger, M. A. Horne, A. Shimony, and A. Zeilinger, Am. J. Phys. **58**, 1131 (1990).
[5] D. Bouwmeester, J.-W. Pan, M. Daniell, H. Weinfurter, and A. Zeilinger, Phys. Rev. Lett. **82**, 1345 (1999).
[6] M. A. Horne, A. Shimony, and A. Zeilinger, Phys. Rev. Lett. **62**, 2209 (1989).
[7] D. M. Greenberger, M. A. Horne, and A. Zeilinger, Phys. Today **46**, 22 (1993).
[8] D. A. Rice, C. F. Osborne, and P. Lloyd, Phys. Lett. A **186**, 21 (1994).
[9] S. M. Barnett, N. Imoto, and B. Huttner, J. Mod. Opt. **45**, 2217 (1998).
[10] A. Zeilinger, M. A. Horne, H. Weinfurter, and M. Żukowski, Phys. Rev. Lett. **78**, 3031 (1997).
[11] N. D. Mermin, Am. J. Phys. **58**, 731 (1990).
[12] J.-W. Pan, D. Bouwmeester, M. Daniell, H. Weinfurter, and A. Zeilinger, Nature (London) **403**, 515 (2000).
[13] P. Walther, J.-W. Pan, M. Aspelmeyer, R. Ursin, S. Gasparoni, and A. Zeilinger, Nature (London) **429**, 158 (2004).
[14] M. W. Mitchell, J. S. Lundeen, and A. M. Steinberg, Nature (London) **429**, 161 (2004).
[15] M. Corona, K. Garay-Palmett, and A. B. U'Ren, Opt. Lett. **36**, 190 (2011).
[16] T. Guerreiro, A. Martin, B. Sanguinetti, J. S. Pelc, C. Langrock, M. M. Fejer, N. Gisin, H. Zbinden, N. Sangouard, and R. T. Thew, Phys. Rev. Lett. **113**, 173601 (2014).
[17] H. Hübel, D. R. Hamel, A. Fedrizzi, S. Ramelow, K. J. Resch, and T. Jennewein, Nature (London) **466**, 601 (2010).
[18] See Supplemental Material at http://link.aps.org/supplemental/10.1103/PhysRevLett.118.153602 for additional experimental details and data, which includes Ref. [19].
[19] D. R. Hamel, L. K. Shalm, H. Hübel, A. J. Miller, F. Marsili, V. B. Verma, R. P. Mirin, S. W. Nam, K. J. Resch, and T. Jennewein, Nat. Photonics **8**, 801 (2014).
[20] D. N. Klyshko, Phys. Lett. A **172**, 399 (1993).
[21] A. V. Belinsky and D. N. Klyshko, Phys. Lett. A **176**, 415 (1993).
[22] J. Brendel, N. Gisin, W. Tittel, and H. Zbinden, Phys. Rev. Lett. **82**, 2594 (1999).
[23] M. Hillery, V. Bužek, and A. Berthiaume, Phys. Rev. A **59**, 1829 (1999).
[24] G. Vallone, P. Mataloni, and A. Cabello, Phys. Rev. A **81**, 032105 (2010).
[25] N. D. Mermin, Phys. Rev. Lett. **65**, 1838 (1990).
[26] G. Svetlichny, Phys. Rev. D **35**, 3066 (1987).
[27] L. K. Shalm, D. R. Hamel, Z. Yan, C. Simon, K. J. Resch, and T. Jennewein, Nat. Phys. **9**, 19 (2012).
[28] J. T. Barreiro, N. K. Langford, N. A. Peters, and P. G. Kwiat, Phys. Rev. Lett. **95**, 260501 (2005).
[29] A. J. Menssen, A. E. Jones, B. J. Metcalf, M. C. Tichy, S. Barz, W. S. Kolthammer, and I. A. Walmsley, following Letter, Phys. Rev. Lett. **118**, 153603 (2017).